Singlet–Triplet Transition Rate Enhancement inside Hyperbolic Metamaterials

Diane J. Roth, Pavel Ginzburg, Liisa M. Hirvonen, James A. Levitt, Mazhar E. Nasir, Klaus Suhling, David Richards, Viktor A. Podolskiy, and Anatoly V. Zayats*

The spontaneous emission process is known to be largely affected by the surrounding electromagnetic environment of emitters, which manifests itself via the Purcell enhancement of decay rates. This phenomenon has been extensively investigated in the case of dipolar transitions in quantum systems, commonly delivering fast decay rates in comparison to forbidden transitions such as high-order multipolar transitions or spin-forbidden, singlet–triplet phosphorescence processes. Here, a decay rate enhancement of almost 2750-fold is demonstrated for a ruthenium-based phosphorescent emitter located inside a plasmonic hyperbolic metamaterial. The standard electromagnetic local density of states description, typically employed for the Purcell factor analysis of dipolar transitions, is unable to account for a photoluminescence enhancement of this magnitude, which is attributed to the interplay between the local density of states and strongly inhomogeneous electromagnetic fields inside the metamaterial. The large available range of spontaneous emission lifetimes reported here enables application of phosphorescent emitters in novel, fast, and efficient light-emitting sources, beneficial for optical communications, quantum information processing, spectroscopy, or bio-imaging.

1. Introduction

The enhancement of the spontaneous emission rates of dipolar emitters, known as the Purcell effect,[1] has been demonstrated in many different material environments, owing to the modification of the local density of electromagnetic states (LDOS) available for the emitters' relaxation.[2] Photonic structures, such as photonic crystals[3] or microresonators,[4] have received a lot of interest in the past thanks to their high quality factors, but their use has been hindered by diffraction limited modal volumes, restricting the enhancement factors. Instead, the use of plasmonic structures, such as nanoantennas[5] or plasmonic cavities,[6] has enabled the confinement of light to subwavelength scales, delivering modal volumes far beyond the diffraction limit. Despite the limitation of the enhancement factors due to the inherent material losses[7] of the plasmonic structures, the resonant character of the enhancement process nonetheless led to rather narrow enhancement bandwidths. Recently, sizeable spontaneous emission rate enhancements using metamaterials, ordered nanostructured media with designed electromagnetic properties, have been achieved. A subclass of metamaterials, namely hyperbolic metamaterials (HMM),[8] has been shown to deliver broadband non-resonant Purcell enhancement, limited by microscopic factors, such as the composite granularity.[9–11] Most of the experimental studies involving hyperbolic metamaterials reported Purcell factors of several tens,[12–15] reaching ≈80 with additional structuring of a metal-dielectric multilayer metamaterial.[16] In nanorod-based hyperbolic metamaterials, decay rate enhancements of dipolar emitters reaching up to 100 were observed, depending on the positioning of the emitters in the unit cell as well as the material losses,[9] and led to emission in both free space and waveguided modes of the metamaterial slab.[15,17]

Spontaneous emission from other atomic transitions has, however, not been extensively investigated, mostly due to their conventionally forbidden character strictly controlled by selection rules. Electric-dipole-forbidden atomic transitions, such as magnetic-dipole transitions, multipolar transitions with orbital angular momentum changes, spin-flip-required, or singlet–triplet transitions, are typically orders of magnitude slower than regular dipolar transitions between selection-rule-allowed states, and therefore are hardly experimentally observable. However, it was recently shown that using highly confined plasmon modes of 2D materials or surface magnon polaritons, these forbidden emission processes can be significantly accelerated and may

Dr. D. J. Roth, Dr. L. M. Hirvonen, Dr. J. A. Levitt, Dr. M. E. Nasir, Prof. K. Suhling, Prof. D. Richards, Prof. A. V. Zayats
Department of Physics and London Centre for Nanotechnology
King's College London
Strand, London WC2R 2LS, UK
E-mail: diane.roth@kcl.ac.uk

Dr. P. Ginzburg
School of Electrical Engineering
Tel Aviv University
Tel Aviv 69978, Israel

Prof. V. A. Podolskiy
Department of Physics and Applied Physics
University of Massachusetts Lowell
One University Ave
Lowell, MA 01854, USA

The ORCID identification number(s) for the author(s) of this article can be found under https://doi.org/10.1002/lpor.201900101

DOI: 10.1002/lpor.201900101

compete with conventional dipolar transitions with emission primarily into plasmonic and polaritonic modes; while the increased local density of electromagnetic states plays an important role in the Purcell effect, strong gradients in highly confined electromagnetic fields are essential for the enhancement of forbidden transitions.[18–21]

In the specific case of phosphorescence, which is a second-order quantum process, emitters typically exhibit lifetimes in the range of milliseconds to seconds,[22] orders of magnitude longer than the common nanosecond lifetimes of fluorescent dyes. This comes from the forbidden nature of the transitions involved in the emission process, including transitions between states of different spin multiplicities such as singlet–triplet transitions. However, the phosphorescence process can be enhanced in organometallic complexes possessing a heavy transition-metal element, favoring spin–orbit coupling interactions. This therefore results in improved quantum yields and shorter lifetimes of the order of 100 s of ns to 10 s of µs,[22] making the phosphorescent transitions experimentally accessible. Here we report on the decay rate enhancement of a singlet–triplet transition in a long lifetime phosphorescent ruthenium-based complex (Ru(dpp)) inside a gold-nanorod-based hyperbolic metamaterial. Large enhancements of the transition rate are observed on smooth gold films and metamaterial-based structures, suggesting the inapplicability of the commonly used Purcell factor for pure dipolar transitions, based on the electromagnetic local density of states modifications only. Embedding the emitters within the hyperbolic metamaterial, realised as an array of vertically aligned gold nanorods, yields the record lifetime reduction of ≈2750-fold at the maximum peak of the measured lifetime distribution (an ≈4800-fold reduction can be estimated at the tail of the lifetime distribution). Theoretical predictions, relying on electromagnetic local density of states, fail to predict such an enormous rate acceleration, instead pointing to the role played by the electromagnetic field gradients between the nanorods forming the array.

2. Results and Discussion

In this study, the decay dynamics of ruthenium-tris(4,7-diphenyl-1,10-phenanthroline) dichloride complex (Ru(dpp), Sigma-Aldrich) dissolved in different solvents, were measured in the vicinity of various plasmonic substrates, employing a time-correlated single photon counting (TCSPC) technique (see Experimental Section). Ru(dpp) is a transition metal complex, which is constituted of a central Ru^{2+} ion surrounded by 3 diphenyl-phenanthroline ligand molecules. Due to the presence of the ligands, these complexes exhibit unique electronic transitions called metal-to-ligand charge-transfer (MLCT) states. These transitions involve a charge transfer from the d-orbitals of the metal (t_{2g}) to the unoccupied π^*_L orbital of the ligands, as represented in the simplified diagram of the molecular orbitals and states of the complex in **Figure 1**a. Following absorption from the ground state (S_0) to the ^{1}MLCT singlet state, fast and efficient intersystem crossing occurs (k_{isc}) and electrons relax to the triplet ^{3}MLCT state. Emission from this triplet state to a singlet ground state is classified as phosphorescence (k_r) and exhibits lifetimes of the order of several microseconds, shorter than usual phosphorescent state lifetimes.[22] This efficient intersystem crossing and reduced lifetime of the triplet excited state is due to the presence of the ruthenium transition-metal ion, inducing spin–orbit interactions and enhancing the probability of the theoretically spin-forbidden triplet to ground-state transitions, therefore increasing the efficiency of the phosphorescence process.[23]

The ruthenium-based emitter was first dissolved in water and then deposited on: a glass substrate; a smooth gold film of thickness 30 nm; and inside a gold-nanorod-based hyperbolic metamaterial (see scanning electron microscopy (SEM) image, Figure 1b). The nanorod array parameters used in this experimental study were ≈250 ± 5 nm length, 50 ± 2 nm diameter, and 100 ± 2 nm center-to-center spacing. More details on the fabrication process of the metamaterial structure are available in the Experimental Section. The extinction spectra of the free-standing nanorod array immersed in water for different angles of incidence of transverse magnetic (TM)-polarized light (Figure 1c) show the presence of two modes associated with the electron motion perpendicular (⊥) and parallel (//) to the nanorods, respectively centered around 530 and 585 nm.[24]

The decay dynamics of the emitters deposited on glass, the gold film, and the nanorod metamaterial are represented in **Figure 2**a. These decays were fitted using an inverse Laplace transform method described in the Experimental Section. In the case of the emitters deposited on glass, the experimental decay is mono-exponential with a component of the lifetime distribution centered around 770 ns (Figure 2b), in good agreement with values found in the literature.[25] The measurements on the gold film and inside the nanorod-based metamaterial exhibit much more complicated decay dynamics compared to that of glass. For emitters placed on the gold film, the dependence of the lifetime on the position and orientation of the emitters with regard to the gold surface led to a multi-exponential decay (Figure 2a,b). The gold-film-modified lifetime distribution is broadened compared to the case of glass and is dominated by a lifetime component centered on 3.7 ns, corresponding to an increase of the decay rate of ≈210. The large span of the lifetime distribution is mainly related to the distance and orientation-dependent distribution of the emitters with regard to the interface but can also be influenced by the level of noise in the experimental data.

In this case, it is shown that the observed decay rate enhancement cannot be explained with the help of the commonly accepted LDOS theory.[2] The dynamics of emitters, modified by the presence of nearby plasmonic surfaces, in particular those of noble metals, is a well understood process. The key contributions leading to the modification of the spontaneous emission lifetime are mainly mirror-reflected waves, the excitation of surface plasmons, and quenching.[26] All these effects can be taken into account in a semi-analytical formula for the spontaneous emission enhancement as described in the Experimental Section. Using this theoretical formulation and the experimentally measured lifetime distribution of the emitter on a glass coverslip, a theoretical prediction of the lifetime distribution on the gold film could be obtained for various depths of optical excitation above the surface. This method takes into account the position of the emitters with regard to the metallic surface and their spatial orientation. As can be seen from the theoretical predictions (Figure 2d), even for a small depth of excitation, the average lifetime enhancement does not even increase by as much as a factor of 10, which is more than an order of magnitude lower than the

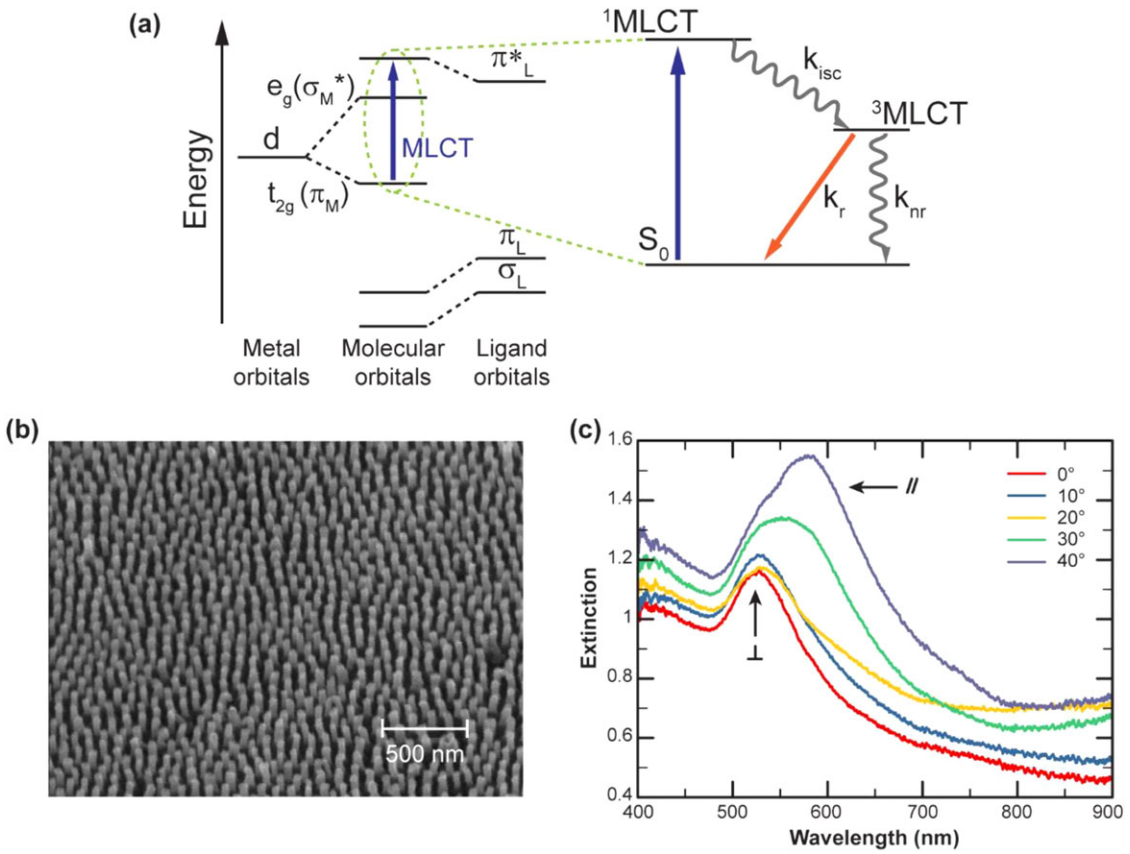

Figure 1. Properties of the ruthenium-based complex and the gold-nanorod-based metamaterial. a) Simplified molecular orbitals and state diagram of the ruthenium-based complex. Energy level positions are not to scale. MLCT stands for metal-to-ligand charge transfer. b) SEM image of a typical nanorod-based metamaterial sample (tilted at 45°). c) Experimental extinction spectra ($-\log T$) of the free-standing nanorod-based metamaterial in water ($n = 1.33$) taken for different angles of incidence of TM-polarized light.

experimentally observed value. It is worth noting that this same fitting procedure was conducted on the lifetime distributions of conventional fluorescent dyes (Alexa, Fluorescein, ATTO dyes) obtained using the same experimental setup, leading to an excellent agreement between theoretical and experimental data for a depth of excitation of 175 nm, verifying the validity of the method.[9]

When deposited inside the metamaterial, the phosphorescent emitter exhibits strongly accelerated decay dynamics, following a multi-exponential profile owing to the random position and polarization of the emitters within the metamaterial. The corresponding lifetime distribution is largely shifted toward shorter lifetimes and shows a maximum peak around 0.28 ns, corresponding to ≈2750-fold reduction of the spontaneous emission lifetime. A reduction of ≈4800-fold can be estimated at the tail of the main peak of the lifetime distribution. The homogenized properties of the metamaterial cannot be directly employed for calculation of the quantum dynamics of emitters, situated inside the structure, due to the finite size of the metamaterial unit cell.[27] However, a comprehensive analysis of the decay rates of emitters inside the nanorod-based metamaterial, taking into account spatial averages, local field corrections, interfaces, and spatial dispersion effects, which has been developed by us previously,[9] has been demonstrated to predict the correct decay rates for widely used dipolar emitters; this theory predicts an averaged spontaneous emission rate enhancement of about 30, also consistent with other reports. However, in the present case, as for a flat gold film, this theoretical description fails to predict the modification of the spontaneous emission lifetime. Therefore, this approach relying on the modification of the LDOS appears to be inapplicable in the case of phosphorescent emission. Photoluminescence spectroscopy of the emitter inside the metamaterial was also performed (Figure 2c), where a slight red-shift of the emission inside the metamaterial is observed with regard to the emitters deposited on glass.

Over the past decades, ruthenium-based emitters have extensively been used as efficient oxygen sensors.[28–30] In the presence of molecular oxygen, dynamic quenching occurring via collisions leads to the de-excitation of the emitter, ultimately reducing its spontaneous emission lifetime.[31] In order to minimize the effect of oxygen in our study, the same experiments were conducted in glycerol, exhibiting a higher viscosity than water and therefore limiting the dynamic quenching process. In this case, a nanorod-based metamaterial sample coated with a thin layer of polymer (7.5 nm), as described in the Experimental Section, was used as an additional material environment. This coating is expected to reduce the emission quenching due to the close proximity of the metallic nanorods to the emitters. The bare nanorod metamaterial sample was fabricated with the same geometrical parameters as the sample used for the emitter in water, while those

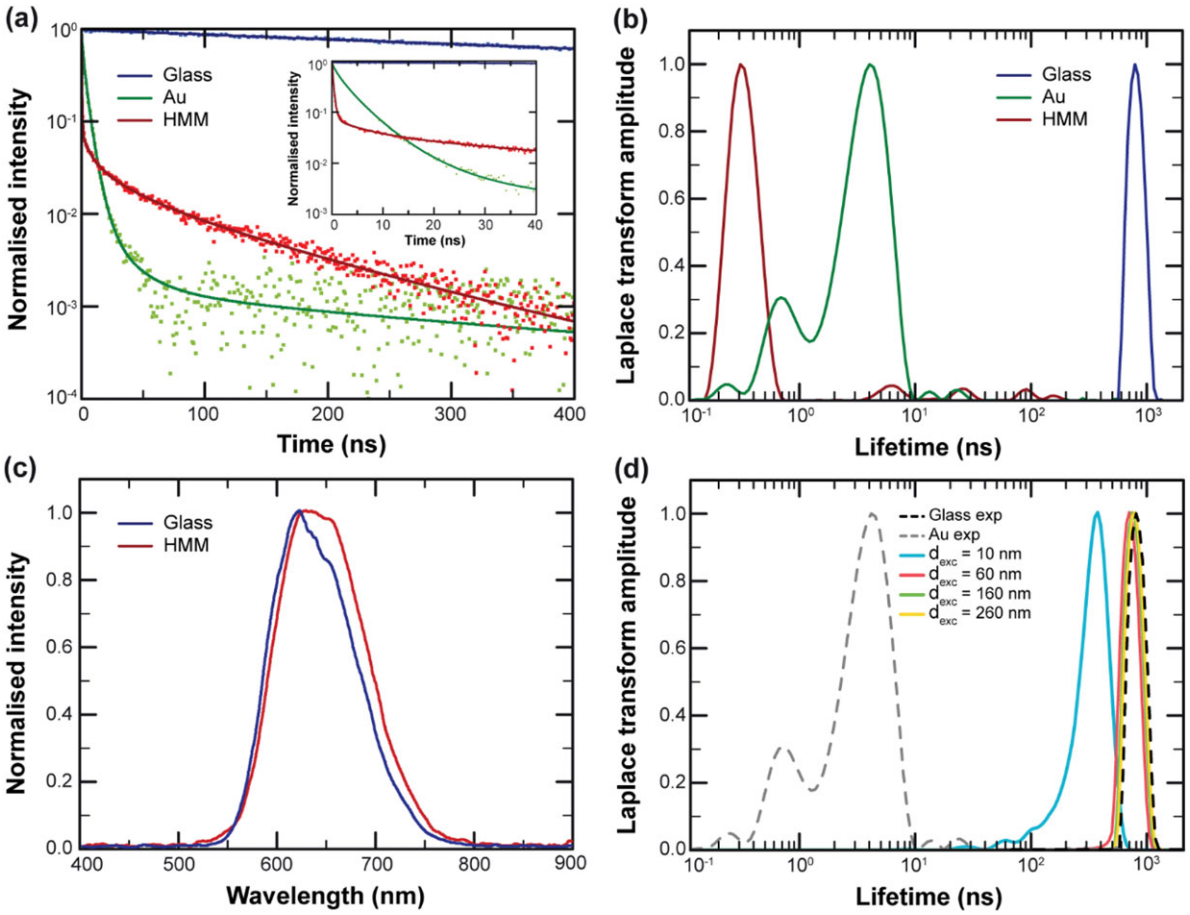

Figure 2. Ruthenium-based complex in water. a) Emission dynamics of Ru(dpp) in water on (blue) a glass substrate, (green) a 30 nm thick gold film, and (red) inside the nanorod-based metamaterial. The dotted lines correspond to the experimental data and the solid lines represent the fits performed using an inverse Laplace transform method. The inset shows the decays on gold and the hyperbolic metamaterial over a shorter timescale. b) Lifetime distributions corresponding to the fits in (a), with the same colour coding. c) Emission spectra of Ru(dpp) in water deposited (blue) on glass and (red) inside the nanorod-based metamaterial. d) Theoretical lifetime distributions above the smooth gold film recalculated from the measured lifetime distributions of the emitters deposited on glass for different depths of excitation (d_{exc}). Dashed lines are experimental data measured on glass and above the gold film, solid lines are the theoretical estimations.

of the coated nanorod metamaterial sample were ≈130 ± 5 nm length, 50 ± 2 nm diameter, and 100 ± 2 nm center-to-center spacing. The extinction spectra of both bare and polymer coated free-standing nanorods immersed in glycerol, for different angles of incidence of TM-polarized light, again show the presence of two peaks (**Figure 3**). In comparison with Figure 1c, an increased splitting between the two modes is observed due to the higher refractive index of glycerol to that of water.[24]

The analysis of the time-resolved measurements show that the decay dynamics of the emitters deposited on glass exhibits a mono-exponential profile, whereas the decay dynamics of the emitters in the cases of the gold film, the bare metamaterial, and the polymer coated metamaterial samples show here again more complicated profiles (**Figure 4**a). In the case of the emitters deposited on glass, the associated lifetime distribution of the complex is centered around 4.4 µs (Figure 4b), in good agreement with values found in the literature.[25] The lifetime distributions of the emitters placed on the gold film, the bare metamaterial, and the coated metamaterial are broadened and strongly shifted toward shorter lifetimes. Considering the position of the maximum of the dominant peak of the lifetime distribution, an ≈980-fold reduction of the lifetime is observed when the emitter is placed near the gold surface and about 2590-fold reduction in the case of the emitters inside the bare metamaterial. A reduction of ≈4600-fold can be estimated at the tail of the main peak of the lifetime distribution for the bare metamaterial. For the coated metamaterial sample, the presence of the polymer shell significantly reduces the decay rate enhancement of the ruthenium-based emitter compared to the bare metamaterial (Figure 4a). The corresponding distribution of lifetimes, represented in Figure 4b, exhibits a maximum around 3.9 ns, leading to a 1130-fold increase of the decay rate compared to the case of glass (an ≈2100-fold increase is observed at the tail of the main peak of the lifetime distribution). This more moderate rate enhancement can be related to the reduced access of the emitters to the field with strongest gradients and/or the prevention of nonradiative quenching typically occurring for emitters in very close proximity to metals, emphasizing the strong dependence of the decay rate on the positioning of the emitters within the metamaterial. Photoluminescence spectroscopy was performed for the emitters

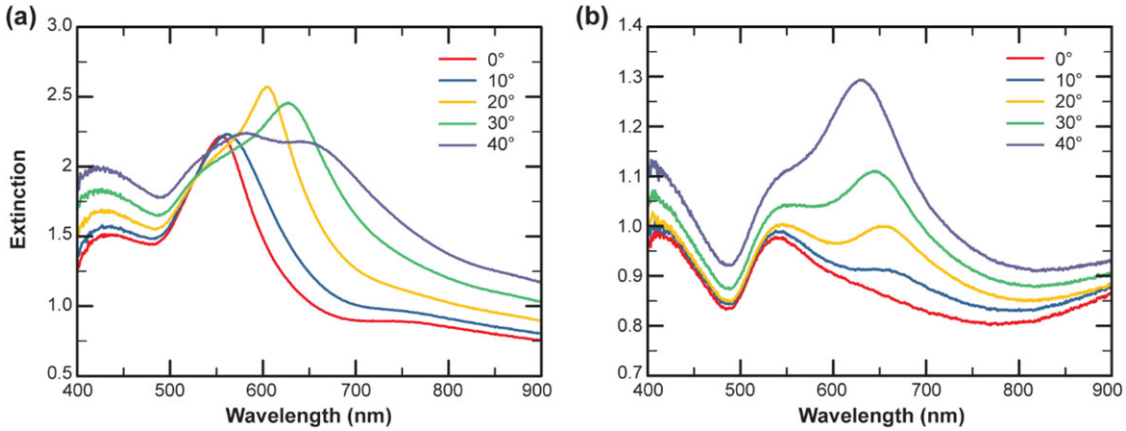

Figure 3. Optical properties of the metamaterial in glycerol. a,b) Experimental extinction spectra (−log*T*) of the bare (a) and the coated (b) free-standing nanorod-based metamaterial in glycerol ($n = 1.47$) taken for different angles of incidence of TM-polarized light.

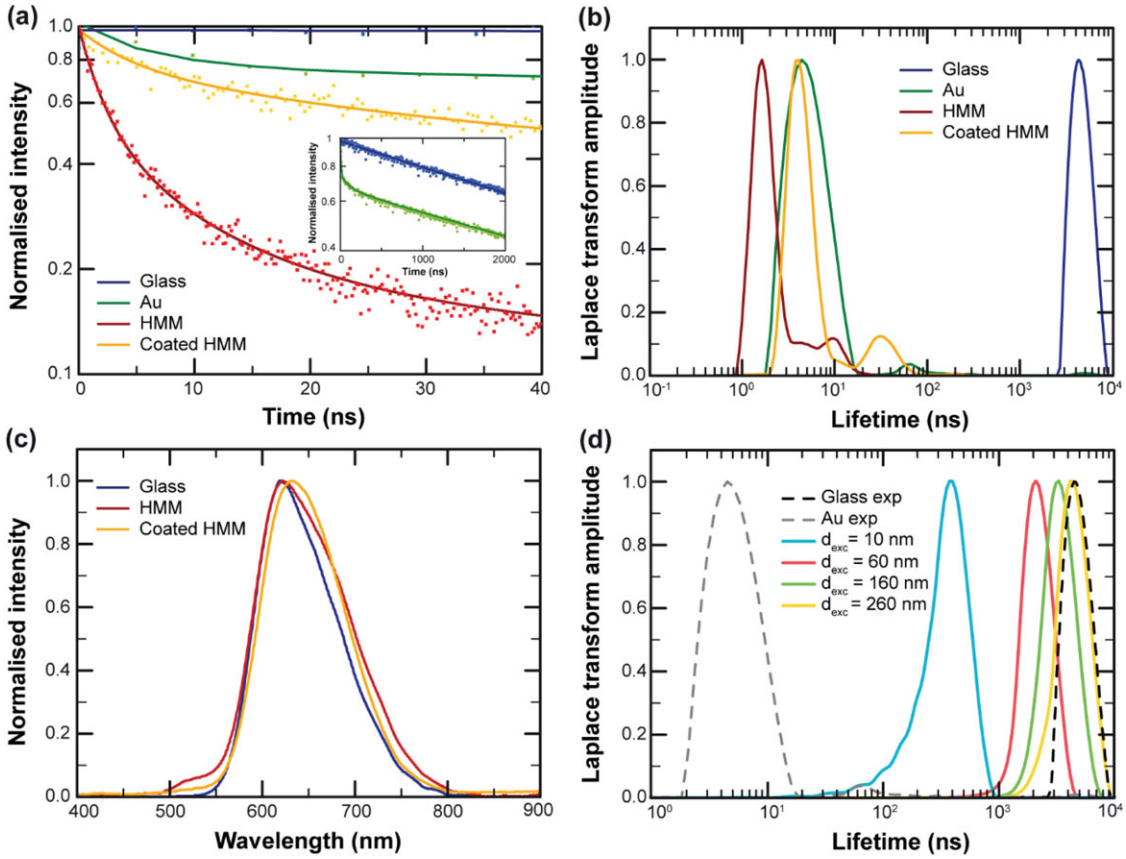

Figure 4. Ruthenium-based complex in glycerol. a) Emission dynamics of Ru(dpp) in glycerol on (blue) a glass substrate, (green) a 30 nm thick gold film, (red) inside the bare nanorod-based metamaterial, and (yellow) inside the polymer coated nanorod-based metamaterial. The dotted lines correspond to the experimental data and the solid lines represent the fits performed using an inverse Laplace transform method. The inset shows the decays on glass and gold on a longer timescale. b) Lifetime distributions corresponding to the fits in (a), with the same colour coding. c) Emission spectra of Ru(dpp) in glycerol deposited (blue) on glass, (red) inside the bare nanorod-based metamaterial, and (yellow) inside the polymer-coated nanorod-based metamaterial. d) Theoretical lifetime distributions above the smooth gold film recalculated from the measured lifetime distributions of the emitters deposited on glass for different depths of excitation (d_{exc}). Dashed lines are experimental data measured on glass and above the gold film, solid lines are the theoretical estimations.

on glass and inside the bare and coated metamaterials as shown in Figure 4c, where the emission spectra inside the metamaterial are here again slightly red-shifted compared to the emitter on glass, owing to the interaction with the nanorods. Using the same method as described in the case of the emitters dissolved in water, a theoretical prediction of the distribution on the gold film was obtained from the experimental distribution on glass for different depths of excitation (Figure 4d). The same conclusion as for the emitters in water can be observed and confirms the inapplicability of the conventional dipolar transition LDOS method for phosphorescence.

3. Conclusion

The decay dynamics of a phosphorescent ruthenium-based complex located in the vicinity of different electromagnetic environments were investigated. By combining the use of an emitter with large spin–orbit coupling and plasmonics, giant enhancements of the singlet–triplet transition rate were demonstrated in the vicinity of plasmonic substrates, including smooth thin gold films and gold-nanorod-based metamaterial structures, which cannot be simply described by the theory used for pure dipolar transitions. While the decay rate enhancement in the case of fluorescence processes has been proven to be theoretically predicted by the LDOS theory, we have shown that the description considering only the LDOS fails in the case of singlet–triplet transitions. For such transitions, the strong gradients of the electromagnetic field need to be taken into account.[18–21] These gradient effects are available in the near-field proximity to the gold film, due to the excitation of surface plasmons by the emitter's radiation, as well as between the nanorods forming the metamaterial. Decay rates up to two orders of magnitude higher than those predicted by the LDOS theory were observed both in the case of the emitter located near the smooth gold film and inside the metamaterial. Recently, several experimental studies on phosphorescent emission enhancement and decay rate manipulation with modified electromagnetic environments were reported. Among them, 320-fold luminescence enhancement in the vicinity of photonic crystals[32] was achieved and Purcell factors of more than 10^3 near plasmonic structures[33] were demonstrated, where the plasmonic systems investigated exhibit inherently strong field gradients related to the formed nanoscale gaps. It should be noted that a good agreement between experimental results and modeling using a theory based on standard dipolar transitions was obtained in ref. [33] for the investigation of a different ruthenium-based dye in a plasmonic gap antenna. Several factors may have however contributed to the dissimilar observations to those of our study, such as the extremely small gaps potentially leading to strong coupling to the gap modes of the system or the specific orientational characteristics of the dipole radiation in the simulations. In addition to these studies, the role of the field gradients and the differences between the rate modifications of dipolar and dipolar-forbidden transitions have also recently been shown theoretically.[34] A similar combination of a high LDOS and a nonuniform field distribution are likely responsible for the observations in this work and in the aforementioned papers. In nanorod-based metamaterials, additionally to the presence of strong field gradients, the interaction between the emitters and the optical orbital angular momentum of the cylindrical surface plasmons propagating along the nanorods might also play a role in the decay rate enhancement.[18] These results show the remarkable potential of hyperbolic metamaterials for the control of spontaneous emission rates over a large range, useful for the design of fast and enhanced light-emitting devices.

4. Experimental Section

Fabrication of the Metamaterial: The nanorod-based hyperbolic metamaterials were fabricated via electrodeposition of gold into a porous anodized aluminum oxide (AAO) template, as described in ref. [35]. Highly ordered pores were obtained using a two-step anodization process in 0.3 M oxalic acid at 40 V. After an initial anodization step, the porous layer formed was etched in a solution of H_3PO_4 (3.5%) and CrO_3 (20 g L^{-1}) at 70 °C, yielding an ordered, indented Al surface. The second step anodization was then performed under the same conditions as in the first step. An etching step in NaOH was then used to achieve pore widening and remove the barrier layer at the bottom of the pores. Gold electrodeposition was subsequently performed with a three-electrode system using a non-cyanide solution. The AAO template was subsequently removed using a mixed solution (1:1) of 0.3 M NaOH and 99.5% ethanol. The polymer coated nanorod sample was prepared using a layer-by-layer deposition of polyelectrolytes.[36] Each polyelectrolyte layer was prepared by alternating the deposition of poly(allylamine hydrochloride) and polystyrene sulfonate. For each deposition step, the plasmonic gold nanorod metamaterial was immersed in a polyelectrolyte solution (10 mg mL^{-1} in 1 mmol L^{-1} NaCl aqueous solution) for 30 min and washed with pure water (18 MΩ) to remove any unbound electrolyte. The layer-by-layer process was initiated with the cationic poly(allylamine hydrochloride) layer in order to facilitate the attachment of the first polyelectrolyte layer to the gold nanorods through amine–gold interactions. Gold films of 30 nm thickness sputtered on similar substrates were also used in these experiments.

Optical Characterization: Angle-resolved transmission spectroscopy was performed using light from a tungsten-halogen lamp polarized and collimated onto the sample. The transmitted light was then collected by an objective lens and coupled to a spectrometer equipped with a CCD camera via a multimode optical fiber.

Time-Resolved Photoluminescence Measurements: Time-correlated single photon counting (TCSPC) was employed to evaluate the decay dynamics of the ruthenium complex. A pulsed diode laser (Hamamatsu PLP-10 470, 200 kHz repetition rate) was used as the excitation source for the measurements on glass and on the gold film, while a pulsed laser beam from a supercontinuum laser (Fianium SC450-2, 20 MHz repetition rate), filtered with a 10 nm bandpass filter centered on 488 nm (ZET488/10×, Chroma) was used for the measurements in the metamaterial. The beam was focused on the sample using a high-numerical aperture oil-immersion objective (100×, NA = 1.3) and the PL signal was collected via the same objective. A 490 nm longpass dichroic mirror and a bandpass filter (620 nm, bandwidth 40 nm) centered on the emission peak of the complex were used for the lifetime measurements.

Photoluminescence Lifetime Data Analysis: Time-resolved measurements were analyzed using an inverse Laplace transform method,[9] allowing the determination of lifetime distributions in different material environments. This method does not require any preliminary estimation of the lifetime distribution and is based on the solution of the equation.

$$I(t) = \int_0^\infty F(\tau) e^{-t/\tau} d\tau \tag{1}$$

where $I(t)$ is the measured decay deconvoluted from the instrumental response function and $F(\tau)$ is the relative weight of the exponential decay components. An iterative fitting procedure was used to obtain stable results due to the ill-defined character of inverse methods.

Quantum Yield Measurements: Quantum yields of the ruthenium complex in water and glycerol were measured using a method developed by de Mello et al.[37] The samples, placed in an integrating sphere, were illuminated using a 470 ± 10 nm LED source. The emitted light was collected by a spectrometer (QE Pro, Ocean optics). Quantum yields of 0.099 and 0.81 were measured for the ruthenium complex in water and glycerol, respectively. This difference in the quantum yield may contribute to the stronger observed increase of the decay rate in the metamaterial for water than glycerol solvent.

Estimation of the Lifetime Distribution of the Ensemble of Emitters Near a Gold Film: A semi-analytical expression for the total decay rate enhancement of a point-like emitter near an interface between two materials was used in order to calculate the distribution of lifetimes near the gold surface, as developed in ref. [9]. Given the experimentally measured lifetime distributions of fluorophores near a glass substrate $F^{\text{exp}}_{\text{Glass}}(\tau)$, the corresponding distribution near a gold film can be derived as

$$F^{\text{Theor}}_{\text{Au}}(\tau) \sim \int_0^{d_{\text{exc}}} \left|\vec{E}_{\text{pump}}(z)\right|^2 Q_{\text{loc}}(z)\, n(z)\, F^{\text{exp}}_{\text{Glass}}\left(\frac{\tau}{\psi(z)}\right) dz \qquad (2)$$

where $\psi(z)$ is the position-dependent polarization-averaged total decay rate enhancement factor near the gold surface (relative to the case of emission near the glass substrate), $|\vec{E}_{\text{pump}}(z)|^2$ is the position-dependent intensity of the excitation light, $Q_{\text{loc}}(z)$ is the emitter's local quantum yield, and $n(z)$ is the distribution density of the emitters along the focal depth, which was assumed to be uniform. The depth of excitation d_{exc} was varied.

Acknowledgements

D.J.R., P.G., and L.M.H. contributed equally to this work. This research was sponsored in part by the US Army Research Office (ARO) (W911NF-12-1-0533 and W911NF-16-1-0261), the Binational Science Foundation (project 2016059), EPSRC (UK), and H2020 ERC project iPLASMM (321268).

Conflict of Interest

The authors declare no conflict of interest.

Keywords

hyperbolic metamaterials, phosphorescence, ruthenium complexes, singlet–triplet transitions, time-correlated single photon counting

Received: March 21, 2019
Revised: June 4, 2019
Published online:

[1] E. M. Purcell, *Phys. Rev.* **1946**, *69*, 37.
[2] L. Novotny, B. Hecht, *Principles of Nano-Optics*, Cambridge University Press, Cambridge, UK **2012**.
[3] P. Lodahl, A. F. Van Driel, I. S. Nikolaev, A. Irman, K. Overgaag, D. Vanmaekelbergh, W. L. Vos, *Nature* **2004**, *430*, 654.
[4] J. P. Reithmaier, G. Sek, A. Löffler, C. Hofmann, S. Kuhn, S. Reitzenstein, L. V. Keldysh, V. D. Kulakovskii, T. L. Reinecke, A. Forchel, *Nature* **2004**, *432*, 197.
[5] T. B. Hoang, G. M. Akselrod, C. Argyropoulos, J. Huang, D. R. Smith, M. H. Mikkelsen, *Nat. Commun.* **2015**, *6*, 7788.
[6] K. J. Russell, T.-L. Liu, S. Cui, E. L. Hu, *Nat. Photonics* **2012**, *6*, 459.
[7] J. A. Schuller, E. S. Barnard, W. S. Cai, Y. C. Jun, J. S. White, M. L. Brongersma, *Nat. Mater.* **2010**, *9*, 193.
[8] A. Poddubny, I. Iorsh, P. Belov, Y. Kivshar, *Nat. Photonics* **2013**, *7*, 948.
[9] P. Ginzburg, D. J. Roth, M. E. Nasir, P. Segovia, A. V. Krasavin, J. Levitt, L. M. Hirvonen, B. Wells, K. Suhling, D. Richards, V. A. Podolskiy, A. V. Zayats, *Light: Sci. Appl.* **2017**, *6*, e16273.
[10] Z. Jacob, I. I. Smolyaninov, E. E. Narimanov, *Appl. Phys. Lett.* **2012**, *100*, 181105.
[11] A. N. Poddubny, P. A. Belov, P. Ginzburg, A. V. Zayats, Y. S. Kivshar, *Phys. Rev. B* **2012**, *86*, 035148.
[12] T. Tumkur, G. Zhu, P. Black, Y. A. Barnakov, C. E. Bonner, M. A. Noginov, *Appl. Phys. Lett.* **2011**, *99*, 151115.
[13] M. Y. Shalaginov, V. V. Vorobyov, J. Liu, M. Ferrera, A. V. Akimov, A. Lagutchev, A. N. Smolyaninov, V. V. Klimov, J. Irudayaraj, A. V. Kildishev, A. Boltasseva, V. M. Shalaev, *Laser Photonics Rev.* **2015**, *9*, 120.
[14] H. N. S. Krishnamoorthy, Z. Jacob, E. Narimanov, I. Kretzschmar, V. M. Menon, *Science* **2012**, *336*, 205.
[15] D. J. Roth, A. V. Krasavin, A. Wade, W. Dickson, A. Murphy, S. Kéna-Cohen, R. Pollard, G. A. Wurtz, D. Richards, S. A. Maier, A. V. Zayats, *ACS Photonics* **2017**, *4*, 2513.
[16] D. Lu, J. J. Kan, E. E. Fullerton, Z. W. Liu, *Nat. Nanotechnol.* **2014**, *9*, 48.
[17] D. J. Roth, M. E. Nasir, P. Ginzburg, P. Wang, A. Le Marois, K. Suhling, D. Richards, A. V. Zayats, *ACS Photonics* **2018**, *5*, 4594.
[18] N. Rivera, I. Kaminer, B. Zhen, J. D. Joannopoulos, M. Soljacic, *Science* **2016**, *353*, 263.
[19] P. K. Jain, D. Ghosh, R. Baer, E. Rabani, A. P. Alivisatos, *Proc. Natl. Acad. Sci. USA* **2012**, *109*, 8016.
[20] J. Sloan, N. Rivera, J. D. Joannopoulos, I. Kaminer, M. Soljacic, *arXiv:1810.06761*, **2018**.
[21] A. Manjavacas, R. Fenollosa, I. Rodriguez, M. C. Jiménez, M. A. Miranda, F. Meseguer, *J. Mater. Chem. C* **2017**, *5*, 11824.
[22] J. R. Lakowicz, *Principles of Fluorescence Spectroscopy*, Springer Science & Business Media, Berlin, Germany **2013**.
[23] M. A. Baldo, D. O'Brien, Y. You, A. Shoustikov, S. Sibley, M. Thompson, S. R. Forrest, *Nature* **1998**, *395*, 151.
[24] N. Vasilantonakis, G. Wurtz, V. Podolskiy, A. Zayats, *Opt. Express* **2015**, *23*, 14329.
[25] L. M. Hirvonen, F. Festy, K. Suhling, *Opt. Lett.* **2014**, *39*, 5602.
[26] G. W. Ford, W. H. Weber, *Phys. Rep.* **1984**, *113*, 195.
[27] P. Ginzburg, A. V. Krasavin, A. N. Poddubny, P. A. Belov, Y. S. Kivshar, A. V. Zayats, *Phys. Rev. Lett.* **2013**, *111*, 036804.
[28] B. D. MacCraith, C. M. McDonagh, G. O'Keeffe, E. T. Keyes, J. G. Vos, B. O'Kelly, J. F. McGilp, *Analyst* **1993**, *118*, 385.
[29] B. Lei, B. Li, H. Zhang, S. Lu, Z. Zheng, W. Li, Y. Wang, *Adv. Funct. Mater.* **2006**, *16*, 1883.
[30] R. I. Dmitriev, D. B. Papkovsky, *Cell. Mol. Life Sci.* **2012**, *69*, 2025.
[31] K. J. Morris, M. S. Roach, W. Xu, J. Demas, B. DeGraff, *Anal. Chem.* **2007**, *79*, 9310.
[32] P. Zhou, D. Zhou, L. Tao, Y. Zhu, W. Xu, S. Xu, S. Cui, L. Xu, H. Song, *Light: Sci. Appl.* **2014**, *3*, e209.
[33] G. M. Akselrod, C. Argyropoulos, T. B. Hoang, C. Ciracì, C. Fang, J. Huang, D. R. Smith, M. H. Mikkelsen, *Nat. Photonics* **2014**, *8*, 835.
[34] A. Cuartero-González, A. I. Fernandez-Dominguez, *ACS Photonics* **2018**, *5*, 3415.
[35] P. Evans, W. R. Hendren, R. Atkinson, G. A. Wurtz, W. Dickson, A. V. Zayats, R. J. Pollard, *Nanotechnology* **2006**, *17*, 5746.
[36] C. Ciracì, R. Hill, J. Mock, Y. Urzhumov, A. Fernández-Domínguez, S. Maier, J. Pendry, A. Chilkoti, D. Smith, *Science* **2012**, *337*, 1072.
[37] J. C. de Mello, H. F. Wittmann, R. H. Friend, *Adv. Mater.* **1997**, *9*, 230.